Title
The Electrostatic Transformer

Authors
Colas, J.
Pripstein, M.
Wenzel, W.A.

Publication Date
1990-02-01

LBL-28511
Preprint

Lawrence Berkeley Laboratory
UNIVERSITY OF CALIFORNIA

Physics Division

Submitted to Nuclear Instruments & Methods A

The Electrostatic Transformer

J. Colas, M. Pripstein, and W.A. Wenzel

February 1990

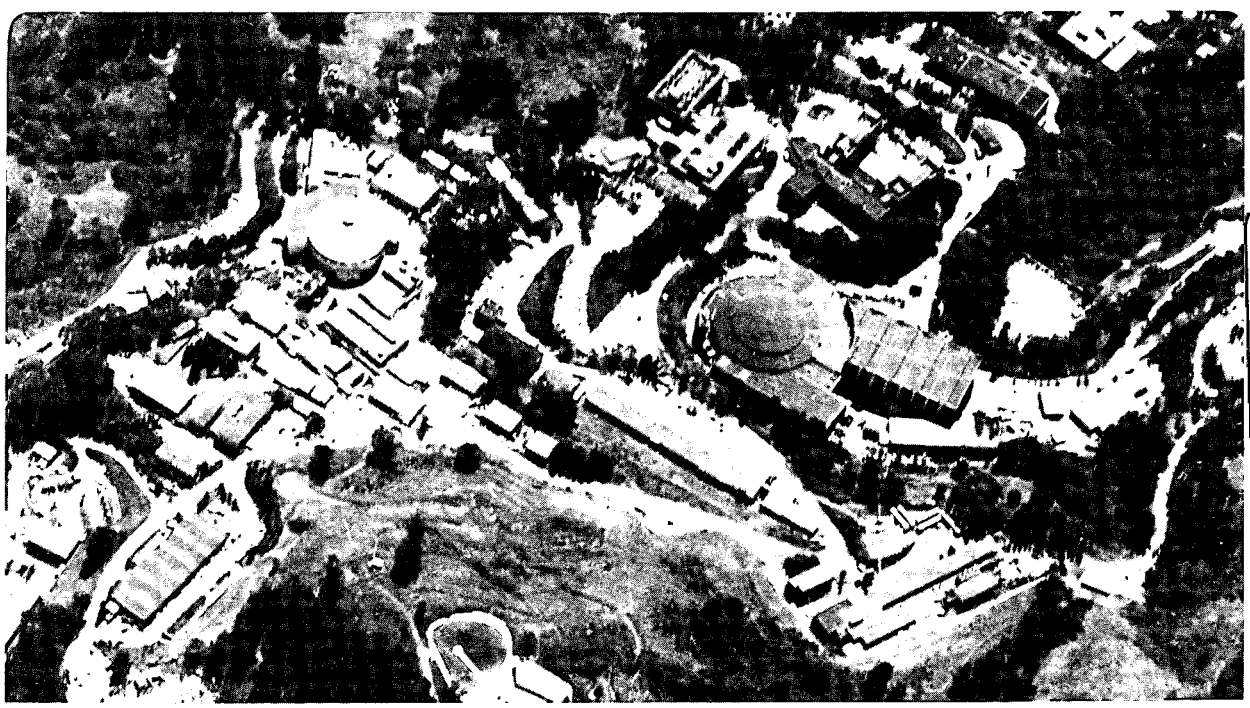

Prepared for the U.S. Department of Energy under Contract Number DE-AC03-76SF00098.

DISCLAIMER

LBL-28511

The Electrostatic Transformer

J. Colas, M. Pripstein, and W.A. Wenzel

Physics Division
Lawrence Berkeley Laboratory
University of California
Berkeley, CA 94720

February 1990

This work was supported by the Director, Office of Energy Research,
Office of High and Nuclear Physics, Division of High Energy Physics
of the U. S. Department of Energy under Contract No. DE-AC03-76SF00098.

THE ELECTROSTATIC TRANSFORMER[1]

J.Colas[2], M.Pripstein and W.A.Wenzel,
Lawrence Berkeley Laboratory, Berkeley, CA 94720

Abstract

The electrostatic transformer (EST) has been developed to match the large capacitance hadronic signal towers of liquid ionization calorimeters to relatively low capacitance, low noise preamplifiers. The intrinsically fast internal impedance transformation by the EST preserves the fast rise time required for effective calorimetry in the high rate environment of the SSC/LHC. Another advantage of the EST over an external ferrite-core transformer (FTC) is that the former is unaffected by the large magnetic field required in most detector configurations. The performance of the EST is limited primarily by crosstalk to neighboring towers, which delocalizes the signal and degrades the signal to noise ratio. In practical applications both these effects can be made small. To aid in the evaluation and design of useful EST's we have studied an aluminum model of a hadronic tower section of typical dimensions. The measurements on the model agree well with calculations using a simple electrical model.

I. LIQUID IONIZATION CALORIMETRY AT THE SSC

In liquid ionization sampling calorimetry the charge is collected using high voltage across uniform sensitive gaps of liquid. These alternate with uniform plates of high Z absorber. Since the signal is proportional to the energy lost, the sensitivity is determined primarily by the geometry, calibration is relatively easy and long term stability is excellent. Other advantages of the ion chamber technology are the short intrinsic rise time of the current pulse and relative insensitivity to radiation damage.

The most significant limitations of the technology derive from the large source capacitance coupled with an intrinsically small ionization signal. The SSC/LHC needs for both fast signal response and excellent energy resolution are especially challenging because the frequent sampling needed for good energy resolution tends to require larger capacitance. Typical hadronic towers extend for two absorption lengths or ≈0.5m in depth with total capacitance ≈10nF. Unless this is reduced, the preamp impedance as well as the inductances associated with cabling, feedthroughs and other connectors can limit significantly the charge transfer time.

Larger capacitance also means more noise. To limit the power and cost of electronics the preamp capacitance per tower must be no more than a few hundred pf; and since the noise is minimized by matching the source capacitance to that of the preamplifier, noise reduction provides a second motivation for reducing the effective output capacitance of the detector.

This work is part of a general effort by the Warm Liquid Calorimetry Collaboration (WALIC)[3] to study room temperature liquids (TMP/TMS) as alternatives to cold liquid argon as sensitive media in sampling calorimeters for the SSC/LHC.

II. TRANSFORMER MATCHING

Alternative designs for a hadronic tower are shown schematically in Figure 1. In both cases the absorbing electrodes are separated by liquid sensitive gaps. Ionization electrons produced by shower particles (dashed diagonal trajectories) are collected with the help of a large voltage gradient (≥10kV/cm). The absorber includes

both the ground plates and the conducting tiles, which define the cross sectional areas of the individual towers.

Otherwise the designs are very different. Figure 1a shows the traditional means of capacitance matching with an external transformer[4]; within the tower all the signal gaps are in parallel. Figure 1b shows an alternative in which subsets of gaps within the tower are in series[5,6]. As seen from the preamplifier this performs an impedance transformation like that of the external ferrite-core transformer (FCT). Because the internal transformation makes direct use of the pulse-energy in the high voltage sensitive gaps, we identify it as an electrostatic transformer (EST).

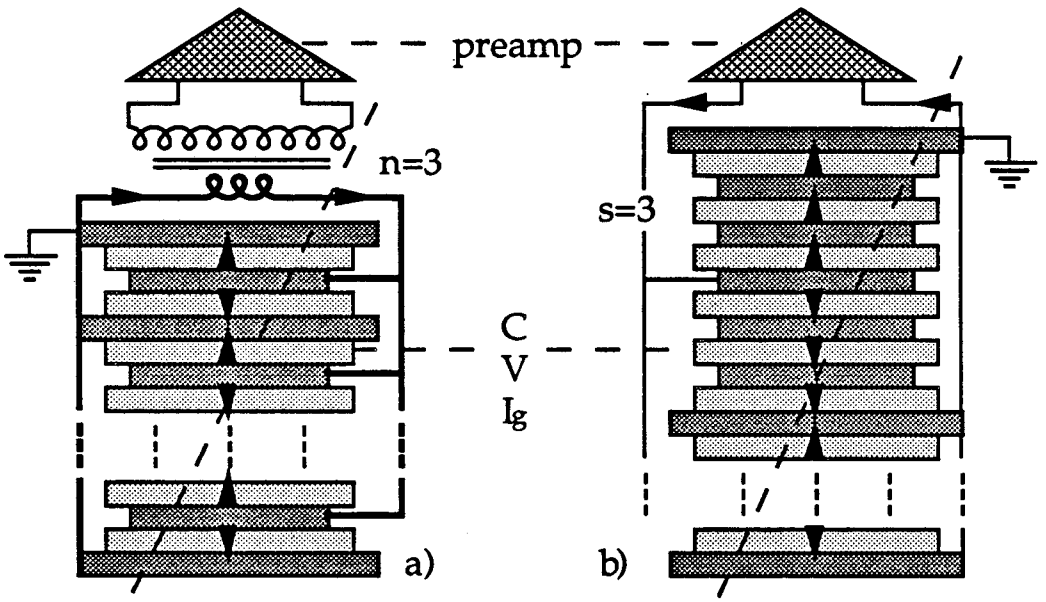

Figure 1. Schematic representation of capacitance matching for a hadronic tower. High voltage connections are not shown. I_g is the ionization current in the g^{th} gap. V and C are the d.c. voltage and capacitance per gap, respectively. The arrows show the directions of current flow. In a) all N gaps are connected in parallel; matching is achieved with a ferrite-core transformer with turns ratio n=3. b) shows an electrostatic transformer with P parallel subtowers of S=3 gaps in series (N=SP).

Table 1 below compares these two types of transformers, each assumed to be ideal.

Table 1. Comparison of ferrite-core and electrostatic transformers used with parallel and series-parallel connected hadronic towers, respectively. Parameters are defined in Figure 1.

Parameter	FCT(Primary)	FCT(Secondary)	EST(Series-Par.)
transformer ratio	n		S
capacitance	NC	NC/n^2	$NC/S^2=PC/S$
signal current	ΣI_g	$\Sigma I_g/n$	$\Sigma I_g/S$
total d.c. voltage	V	----	SV

As an example of the use of the EST, a tower with 40 gaps of 250pf each has a total capacitance of 10nF if all gaps are connected in parallel, but only 0.4nF if there are 8 parallel sets of 5 gaps each in series.

Table 1 implies that the d.c. voltages in adjacent gaps of the EST are connected in series. This is conceptually straightforward, but requires very high voltage for an EST of large S. In various alternative designs[5] the gaps are decoupled individually,

so that the maximum voltage is no greater than the constant voltage V across each gap. The example shown in Figure 2 uses resistively decoupled high voltage on all but the signal tiles, which are at d.c. ground. Signal decoupling uses the capacitance between tiles on opposite sides of the insulators. The voltage difference across each insulator is VS/(S-1).

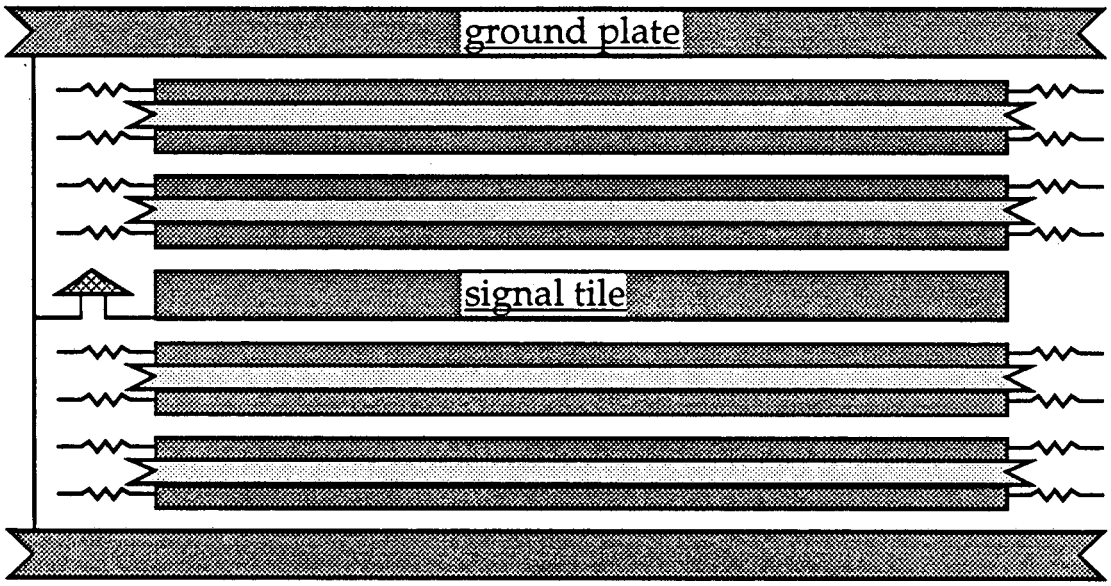

Figure 2. Schematic of two subsections of tower with an electrostatic transformer of ratio S=3. Absorbing signal tile is at d.c. ground. High voltages, decoupled by large resistances, are supplied to the half-tiles, which are separated by thin insulating layers.

III. SIGNALS FROM HADRONIC TOWERS

The small signals from the gaps of the relatively large volume (≥10 liter) hadronic towers must be summed and transported to preamplifiers which are not necessarily close to the source.

A. Ionization current and signal risetime.

Figure 3a shows the time dependence of the electron current in a uniformly illuminated calorimeter gap. In liquid argon the drift velocity is nearly independent of, and in the organic liquids (TMP, TMS) it is nearly proportional to the voltage gradient. For TMP or TMS at the SSC/LHC, the charge collection time T will be ≤100ns. Because the drift of free electrons begins instantaneously, the intrinsic risetime of the ionization current pulse is very small. Preserving this valuable feature in the amplified signal, however, poses some severe challenges for hadronic towers of large capacitance[4][6].

Figures 3b and 3c show the signal paths for the FCT and the EST. The capacitive feedback of the preamp gives a resistive input impedance R_a[4] to damp the signal current with time constant τ. Without a transformer an NC=10nf tower would need a 2.5 ohm preamp input resistance for a pulse rise time $2\tau \approx 50$ns (10-90%). If an FCT is used the signal rise time is especially vulnerable to inductance associated with ganging, connectors and transformer leakage in the large capacitance primary circuit ($L_{crit}=R^2C/4=19$nHy). For simplicity we neglect the L's, but include C_s, the stray capacitance of the transformer secondary. For the FCT and EST:

$$\tau_{FCT}=R_a[(C_S+C_x)/n^2+C_a+C_s] \quad (1)$$
$$\tau_{EST}=R_a(C_S+C_x+C_a)$$

where $C_S=NC/S^2$ (S=1 for FCT), and C_x includes signal ganging and, depending on the configuration, other capacitances external to the tower. In the Helios experiment[7] an FCT at the tower output is used to match the tower capacitance to a low capacitance preamp. If the FCT and preamp are connected to the tower by a transmission line which is short, i.e., with transit time $t_t<<\tau$, then C_x includes the transmission line capacitance $C_t=t_t/R_t$ (see Figure 3). If for the FCT(EST) $n^2R_t \geq R_a (R_t \geq R_a)$ then $C_t<<C_S$, and the transmission line does not greatly affect the design and operation.

An important limitation of the FCT, however, is that it won't work in high magnetic fields. If a long transmission line ($t_t \geq \tau$) is used for this reason and/or to make the preamps more accessible for service, then the signal risetime is preserved only if the transmission line is terminated; i.e., $R_t=R_a$. This condition provides a simple scaling law for the transmission line capacitance; i.e., $C_t/C_\tau=t_t/\tau$, where $C_\tau=C_S(1+x)$ is the relevant capacitance on the tower side of the transmission line, and we define $x=C_x/C_S$. For the NC=10nF tower with τ=25ns, R_{tFCT}=2.5 ohms; for an S=5 EST R_{tEST}=62.5 ohms, in a much more convenient range.

For the termination to be effective it is necessary also that C_a not be too large; i.e., for the EST, $R_aC_a<<\tau$; for the FCT, $R_aC_a(1+s)<<\tau$, where $s=C_s/C_a$.

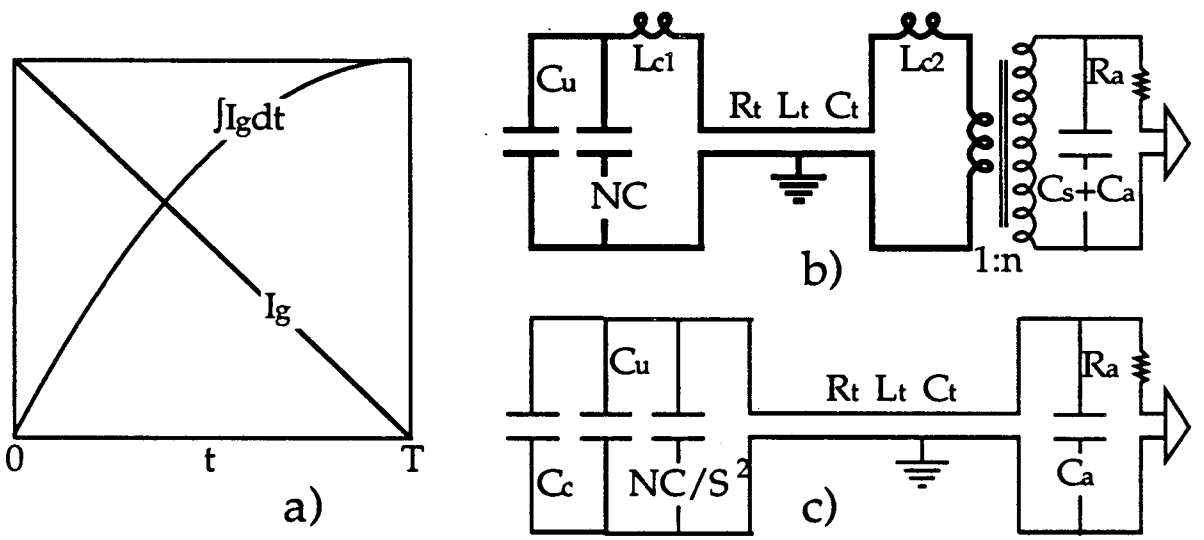

Figure 3. a) shows the ionization current and its integral from a sensitive gap uniformly illuminated at t=0. T is the charge collection time. b) shows schematically the components which can contribute significantly to the charge transfer time if an FCT is used for capacitance matching at the preamp. NC is the paralleled tower-gap capacitance, C_u, C_t, and C_s are for the internal signal ganging line, the transmission line and the stray capacitance of the FCT, respectively. C_a is the input capacitance and R_a the input resistance of the preamp. Bold lines indicate large signal currents; the L_c's are stray inductance from feedthroughs, signal connections and transformer leakage. High voltage decoupling capacitors are not shown. c) shows the corresponding parameters for the EST, for which C_c is the crosstalk contribution to the output capacitance.

B. Signal ganging

In order that the tower gaps be sampled uniformly, the differences in the signal arrival times must be small compared with the pulse shaping time. If we assume that, as a practical design feature, the tower signal is extracted from one end, then we require that $10ns \approx t_g << 2\tau \approx 50ns$, where t_g is the transit time of the signal ganging line. We require also, to limit the capacitance, that the ganging line capacitance is a small fraction g of C_S, then all the ganging line parameters are effectively determined by g, C_S, the dielectric constant ε, the tower depth l and the velocity of light v. For the unloaded (subscript u) and capacitatively loaded (g) ganging line these are:

$$C_u=gC_T;\ t_u=(l/v)(\varepsilon)^{1/2};\ L_u=(t_u)^2/C_u=(l/v)^2(\varepsilon/gC_S);\ R_u=(l/vgC_S)(\varepsilon)^{1/2} \qquad (2)$$
$$C_g=C_S(1+g);\ t_g=t_u[(1+g)/g]^{1/2};\quad L_g=L_u;\qquad R_g=R_u[g/(1+g)]^{1/2}$$

For $\varepsilon=2$; g=0.1, l=0.5m, we find t_g=7.8ns; $L_g(nHy)=56/C_S(nF)$; $R_g(ohms)=7.1/C_S(nF)$. Hence, independent of tower area or choice of FCT or EST, an acceptably small transit time is achieved with only a 10% increase in tower capacitance. But for a 10nF tower the ganging-line inductance for an FCT is a very low 0.1nHy/cm.

C. Effect of crosstalk on tower output capacitance

Figure 4 shows schematically the sources of crosstalk between a central and eight surrounding towers. A fraction of the charge produced in each central gap is coupled to the four side towers, which are similarly coupled to the corner towers.

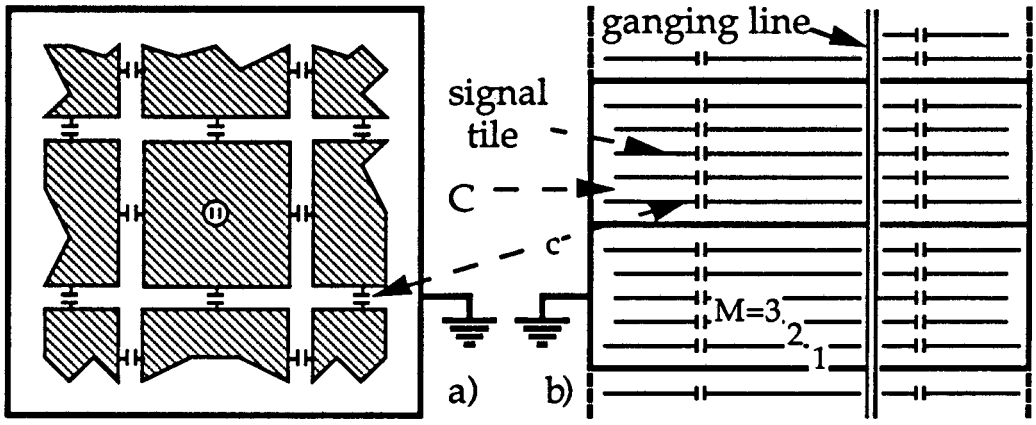

Figure 4. Plan and elevation schematics showing sources of crosstalk between towers of an EST with S=3. Each calorimeter module of many towers is in a grounded container. M is the gap number within a subtower; C is the capacitance of each gap, and c is the coupling, assumed to be constant, of each tile to that of a side tower. Within each tower the signal tiles are summed along a low impedance ganging transmission line, shown here for the central tower only.

For an EST the tower output capacitance C_o includes three important terms:

$$C_o=C_S+C_c+C_u=C_S(1+k+g) \qquad (3)$$

where $C_c=kC_S$ is from crosstalk and $C_u=gC_S$ is discussed in III.*B.* above. Table 2 gives an exact calculation of k for central and side towers (i.e., ignoring presence of

corners). The first order (in c/C) expression for C_c gives $k=(Kc/6C)(2S^2+1)$, valid for $k\leq 0.5$. For $k\geq 0.5$, the most interesting range, a good fit is obtained with $k=S(Kc/6C)^{1/2}$.

Table 2. Crosstalk fraction, $k=C_c/C_S$ for central and nearest-neighbor towers.

S	(Kc/6C)=	0.01	0.02	0.03	0.04
1		0.030	0.059	0.088	0.117
2		0.087	0.168	0.245	0.317
3		0.175	0.327	0.459	0.576
4		0.287	0.510	0.690	0.842
5		0.412	0.699	0.915	1.087
6		0.545	0.882	1.121	1.304
7		0.679	1.053	1.305	1.494
8		0.809	1.210	1.470	1.659
9		0.935	1.354	1.616	1.805
10		1.054	1.484	1.747	1.934

D. Effect of crosstalk on gap efficiency and preamp noise

Crosstalk distributes the signal among neighboring towers. If the tiles are coupled only to neighboring tiles, the total signal charge is conserved among all towers; but the signal of each tower depends on the source-gap and varies with time. For source-charge Q_{SM} deposited at time t=0 in the M^{th} gap of a subtower of S gaps the sum of all tower currents is:

$$I_{aSM}(t) = (Q_{SM}/S\tau)e^{-t/\tau} \qquad (4)$$

where τ is defined in (1). To first order in c/C the current $i_{aSM}(t)$ in a side tower is:

$$i_{aSM}(t) \approx I_{aSM}(t)(c/6C)[(S^2-1-3M^2+3M)+(2S^2+1)(1-t/\tau)/(1+x)] \qquad (5)$$

The corresponding integrated preamp output charges are:

$$Q_{aSM}(t) = (Q_{SM}/S)(1-e^{-t/\tau}) \qquad (6)$$
$$q_{aSM}(t) \approx (Q_{SM}/S)(c/6C)[(S^2-1-3M^2+3M)(1-e^{-t/\tau})+(2S^2+1)(t/\tau)e^{-t/\tau}/(1+x)]$$

where x is defined in III.*A.* above. The charges in the central and side towers are:

$$Q_{aSM\text{-}cent}(t)=Q_{aSM}(t)-Kq_{aSM}(t) \qquad q_{aSM\text{-}side}(t)=q_{aSM}(t) \qquad (7)$$

The M-independent term of $q_{aSM}(t)$ has the same sign as $Q_{aSM}(t)$, its amplitude is reduced by the external capacitance x, and it vanishes at $t=\infty$. The M-dependent term is independent of the external capacitance, has a time dependence similar to that of $Q_{aSM}(t)$, and vanishes in the average over M. This last feature is general, a direct consequence of the tower symmetry; i.e., if all gaps are uniformly excited, no net charge is produced on the internal tiles, and there is no crosstalk.

Important consequences of this average condition are first, that τ does not depend on C_c, although the latter can be a significant part of C_o; and second, that the effect of the crosstalk on preamplifier noise depends on the application. When the tower signals are separately recorded, crosstalk related noise is included, because the

gap signals are incoherent. But if, as is common, many tower signals are summed coherently for a trigger, the coherent noise among these cancels.

The gap-efficiency E_{SM} for each gap is defined to be the normalized charge output from the central tower at t=∞ divided by the total charge from all towers.

$$E_{SM} = 1-Kq_{aSM}(\infty)/Q_{aSM}(\infty) \approx 1-(Kc/6C)(S^2-1-3M^2+3M) \qquad (8)$$

The first form on RHS is general; the last, from (6), is to first order in c/C.

For an arbitrary time dependent source-function the time dependent preamp charges are obtained by folding. Figure 5 shows examples for triangular distributions (Figure 3a) of different durations.

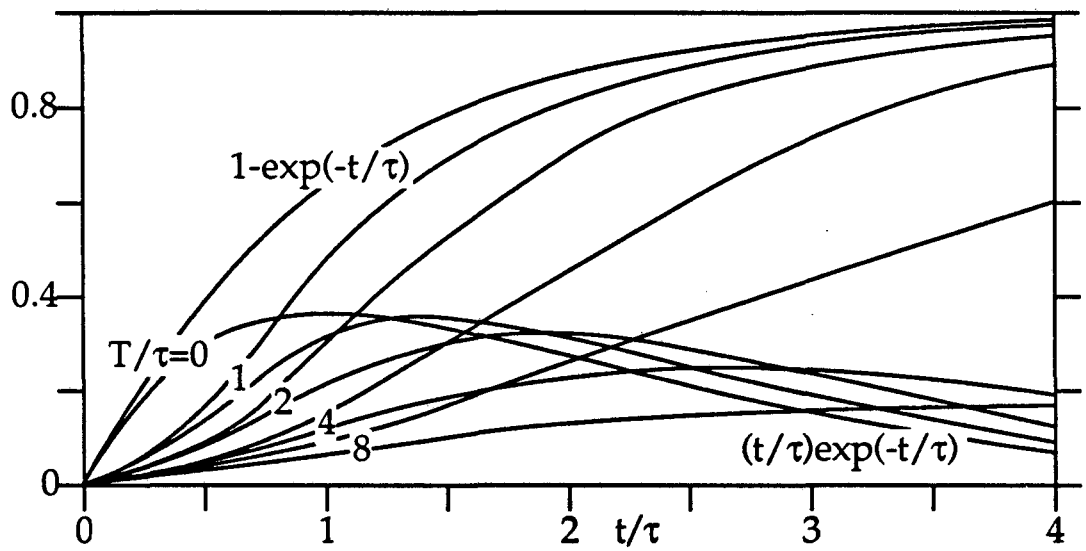

Figure 5. Time dependence of terms describing crosstalk-charge for triangular source functions (Figure 3a) of length T. τ is the time constant defined in (7). Amplitudes are unnormalized.

IV. MODELS OF EST

To evaluate more carefully the electrical and mechanical properties of a calorimeter based on the EST, we have used both mechanical-electrical models and computer-simulation.

A. Aluminum model and computer simulation program SPICE

Figure 6 shows an aluminum model of nine towers assembled inside a grounded box. The central tower was surrounded by four nearest neighbors (sides) and four next nearest neighbors (corners). The dimensions of the aluminum tiles were 6"x6"x3/8". Within the towers the (air) gaps between tiles were set at 0.078" by ceramic spacers.

In each tower the signal from the central tile, which collects charge from both subtowers, was accessible on a rod in a vertical hole through the upper subtower. With access from the top the numbers of tiles between each signal tile and the two ground plates which formed the top and bottom boundaries were changed to vary S. For S=5 (10 gaps), the maximum available, the total depth was approximately one-

fourth that of a high-Z tower of two absorption lengths thickness. The crosstalk capacitance c was varied by changing the tower spacing, which was either 0.125" or 0.25" of air.

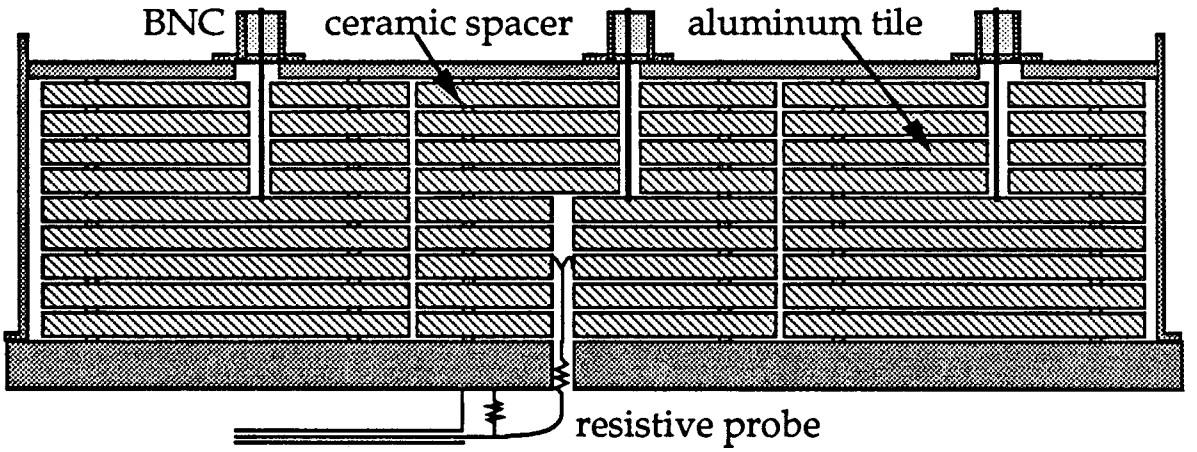

Figure 6. Assembly of the nine-tower aluminum model for S=5. Dimensions are given in the text.

The source current waveform was triangular, of total length 100ns and risetime ≤10ns (Figure 3a). In practice the probe current flowed between a given tile and ground; the effect of a current source in a single gap was obtained from differences. For a variety of conditions the time dependent integrated charge was detected using charge sensitive integrating preamps[8] of 50 ohms nominal input impedance. These monitored the central tower and one other; the seven towers without preamps were terminated in 50 ohms. The measurements were made from photographed traces of a Tektronix 475A Oscilloscope.

Examples of the two crosstalk terms [$q_{aSM}(t)$ in (6)] are illustrated in Figure 7, which shows the charges on the central and one side tower when all gaps or a single gap are excited.

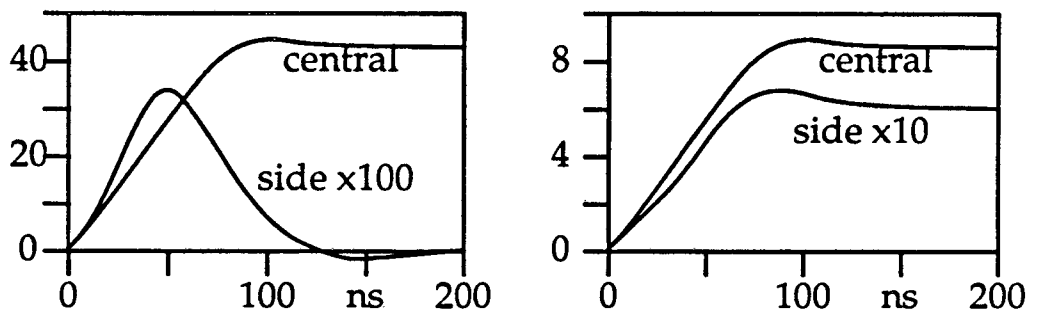

Figure 7. Observed time dependent integrated output currents from the central and a neighboring (side) tower for S=4. and Kc/6C=0.0158. In the left figure all gaps (M=1-4) are excited; at the right only one gap (M=1) is excited. The relative amplitudes are preserved in the vertical scales.

Figure 8 shows the configuration for the simulation program SPICE. The coupling capacitance c was calculated from first principles, i.e., from tower spacing and tile areas. The simulation includes only the central and side towers, omitting crosstalk to the corners and to the surrounding ground box. With large gaps around the outside, the latter effect is negligible. Measurements on the aluminum model for the closest tower spacing (1/8") show that for this 'worst case' the signals from the

corner towers are ≈10% of those from the side towers. Without the next nearest neighbors in the simulation, therefore, the total crosstalk charge decreases by ≈1%.

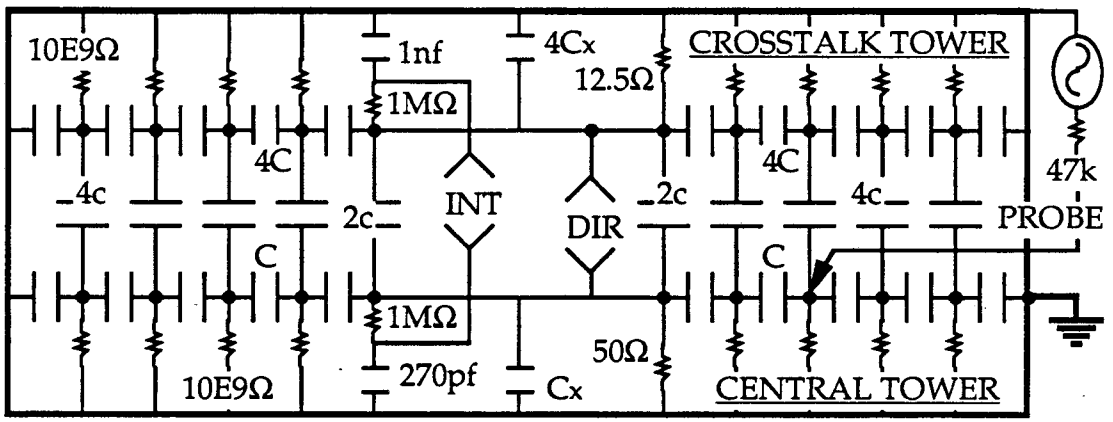

Figure 8. Equivalent circuit used in SPICE calculations for transformer ratio S=5. The crosstalk coupling, stray capacitance and the tower and preamp parameters are combined for the K(=4) nearest neighbors. C_x is the external (including preamp) capacitance. The input voltage pulse on the PROBE is triangular. The voltages at DIR are proportional to the input currents to the preamps. INT voltages are proportional to the outputs from perfect integrating preamps.

B. Comparisons of measurements and SPICE calculations

Table 3 compares measurements on the aluminum model with SPICE calculations; these are generally in excellent agreement. The agreement in the gap-efficiency E_{SM} measurements shows that the tile to tile couplings are relatively

Table 3. Comparison for S=3 and 5 and for tower spacings of 1/8" and 1/4" of measurements on the aluminum model with calculations using SPICE. The source current is shown in Figure 3a; measured and calculated parameters are defined in the text. K=4; C=100pf; normal sampling time =200ns.

tower spacing		1/8"(Kc/6C=0.0317)		1/4"(Kc/6C=0.0158)	
	M	meas.	calc.	meas.	calc.
S=5:					
output capacitance C_O(pf)		85	84	69	69
gap efficiency E_{SM}	1	0.56	0.56	0.72	0.72
	2	0.65	0.65	0.76	0.78
	3	0.82	0.83	0.88	0.92
	4	1.15	1.20	1.12	1.12
	5	1.81	1.76	1.52	1.46
transient-peak time(ns)	1-5	35	41	40	43
normalized amplitude	1-5	0.054	0.034	0.032	0.019
S=3:					
output capacitance C_O(pf)		104	104	90	89
gap efficiency E_{SM}	1	0.79	0.80	0.87	0.89
	2	0.94	0.94	0.95	0.97
	3	1.27	1.26	1.18	1.14
transient-peak time (ns)	1-3	70	72	70	71
normalized amplitude	1-3	0.022	0.017	0.013	0.009

uniform. During the time between the source pulse and normal sampling (200ns), a few per cent of the initially transferred charge was reclaimed by the resistive input PROBE. Since this effect is M-dependent, it distorts the gap efficiencies in the Table; by correcting for this and summing the signal from all nine towers, we find that charge is conserved to ≈1%. The measurements of tower output capacitance C_o include some stray capacitance. Known contributions of ≈ 6pf from the signal rod and BNC output connector are included in the calculations, which agree embarrassingly well with the measurements.

External capacitance was added in parallel with the inputs to the preamps in order to bring the time constant τ of the system into a range appropriate for realistic towers four times as deep. The crosstalk transient term, therefore, was suppressed by relatively large values of x (≈ 6-8). Measurements in the Table are given only for full subtower excitation (all gaps), which maximizes the visibility of this term (Figure 7).

V. CHARGE DELOCALIZATION BY CROSSTALK

Although the signal charge from a tower is on the average proportional to the charge released in that tower, the M-dependence of the gap efficiency E_{SM} means that random fluctuations in the gap-excitations will introduce uncertainties in the transverse charge distribution. From (8) the $t=\infty$ output charges in all towers Q_{aS} and in all side towers Kq_{aS} produced by charges Q_{SM} in the gaps of the central tower are:

$$Q_{aS} = \Sigma\, Q_{SM}/S \qquad Kq_{aS} = \Sigma\, Q_{SM}(1-E_{SM})/S \tag{9}$$

where the sums are over M. Assuming that on the average Q_{SM} and fluctuations δQ_{SM} are independent of M with average values $\langle Q_{SM}\rangle = Q$ and $\langle \delta Q_{SM}\rangle = 0$, we obtain from (9), $\langle Q_{aS}\rangle = Q$, $\langle q_{aS}\rangle = 0$ and:

$$(Kq_{aS}/Q_{aS})_{rms} = (\delta Q/Q)(1-E_{SM})_{rms}/S^{1/2} = F(S)\delta Q/Q \tag{10}$$

where we define $F(S) = (1-E_{SM})/S^{1/2}$ and $\delta Q = \delta Q_{SMrms}$. Exact (without the corner towers) calculations of F(S) are given in Table 4. For $k \geq 0.5$, $F(S) \approx k/6$ (see Table 2). For S=5 and Kc/6C=0.02, (E_{55}/E_{51}=2.3), Table 4 gives F(S) = 0.143; i.e., if $\delta Q/Q \approx 0.5$, only 7% of the charge is delocalized; less than 2% appears in each side tower.

Table 4. Delocalization of charge by crosstalk. Tabulation is of $(1-E_{SM})_{rms}/S^{1/2}$ with $1 \leq M \leq S$.

S	(Kc/6C)	0.01	0.02	0.03	0.04
1		0	0	0	0
2		0.020	0.039	0.057	0.074
3		0.040	0.075	0.106	0.134
4		0.061	0.111	0.151	0.185
5		0.082	0.143	0.189	0.226
6		0.102	0.170	0.220	0.258
7		0.121	0.194	0.244	0.281
8		0.138	0.213	0.263	0.299
9		0.153	0.229	0.278	0.313
10		0.166	0.242	0.290	0.324

VI. CONCLUSIONS

The electrostatic transformer is competitive with ferrite-core transformers in reducing the large capacitances inherent in the hadronic towers needed for SSC calorimetry. Advantages of the EST are that it can preserve the intrinsically fast rise of the ionization pulse, that it is insensitive to magnetic fields and that for preamps located far from the towers it matches a transmission line of convenient impedance. EST performance is degraded primarily by crosstalk between neighboring towers, which delocalizes the signal from the tower of origin. For practical cases this effect is estimated to be small.

Both mechanical and electrical properties of the EST have been studied by testing an aluminum model of nine short towers with transverse dimensions typical of hadronic towers for the SSC/LHC. The performance of the towers is quantitatively predictable from a few geometrical parameters including volume, transformer ratio (number of gaps in series) and the spacing between neighbors. The agreement with electrical measurements has shown that the performance of an EST can be predicted using a simple electrical circuit like the one in Figure 8, which can be computed accurately by SPICE or other methods.

The fabrication and operation of the model have revealed some of the problems of tower and module assembly and signal ganging. Tests are underway using a model with towers of full depth.

References

[1]. This work was supported by the Director, Office of Energy Research, Office of High and Nuclear Physics, Division of High Energy Physics of the United States Department of Energy under Contract No. DE-A C03-76SF00098
[2]. Permanent address: L.A.P.P., Annecy-le-Vieux, 74019, France.
[3]. LBL Group A Physics Note #971, 9/87.
[4]. V. Radeka and S. Rescia. Nucl. Instr. Meth. in Phys. Res., A265 (1988) 228-242
[5]. J.Colas and W.A.Wenzel. "Electrostatic Transformers for Large Towers". LBL-27236. Presented at the Workshop on Calorimetry for the SSC, Tuscaloosa, AL, March 13-17, 1989, and to be published in the Proceedings.
[6]. J. Colas. "Speed of Response, Pile-up, and Signal to Noise Ratio in Liquid Ionization Calorimeters". LBL-27328. Presented at the Workshop on Calorimetry for the SSC, Tuscaloosa, AL, March 13-17, 1989, and to be published in the Proceedings. Also, LAPP-EXP-89-13, November, 1989. Submitted to the proceedings of the ECFA Study Week on Instrumentation for High Luminosity Hadron Colliders, held in Barcelona, Spain, September 14-21, 1989.
[7] D. Zilzinger et al. "The Helios Uranium Liquid Argon Calorimeter." In preparation, CERN, 1989.
[8] D.A.Landis, R.S.Adachi, N.W.Madden and F.S.Goulding. IEEE Transactions in Nuclear Science, Vol. NS-29, No. 1, February, 1982. p573.

LAWRENCE BERKELEY LABORATORY
UNIVERSITY OF CALIFORNIA
INFORMATION RESOURCES DEPARTMENT
1 CYCLOTRON ROAD
BERKELEY, CALIFORNIA 94720